

Growth Kinetics and Microstructure Evolution of Intermediate Phases in MoSi₂-Si₃N₄-WSi₂/Mo Diffusion Couples

Houan Zhang, Yu Huang, Jia Lin, Ying Chen, and Siyong Gu

(Submitted August 2, 2016; in revised form November 5, 2016; published online December 21, 2016)

The growth kinetics and silicon diffusion coefficients of intermediate silicide phases in MoSi₂-3.5 vol.% Si₃N₄-5.0 vol.% WSi₂/Mo diffusion couple prepared by spark plasma sintering were investigated in temperatures ranging from 1200 to 1500 °C. The intermediate silicide phases were characterized by x-ray diffraction. The microstructures and components of the MoSi₂-Si₃N₄-WSi₂/Mo composites were investigated using scanning electron microscope with energy-dispersive spectroscopy. A special microstructure with MoSi₂ core surrounded by a thin layer of (Mo,W)Si₂ ring was found in the MoSi₂-Si₃N₄-WSi₂ composites. The intermediate layers of Mo₅Si₃ and (Mo,W)₅Si₃ in the MoSi₂-Si₃N₄-WSi₂/Mo diffusion couples were formed at different diffusion stages, which grew parabolically. Activation energy of the growth of intermediate layers in MoSi₂-3.5 vol.% Si₃N₄-5.0 vol.% WSi₂/Mo diffusion couple was calculated to be 316 ± 23 kJ/mol. Besides, the hindering effect of WSi₂ addition on the growth of intermediate layers was illustrated by comparing the silicon diffusion coefficients in MoSi₂-3.5 vol.% Si₃N₄-5.0 vol.% WSi₂/Mo and MoSi₂-3.5 vol.% Si₃N₄/Mo diffusion couples. MoSi₂-3.5 vol.% Si₃N₄-5.0 vol.% WSi₂ coating on Mo substrate exhibited a better high-temperature oxidation resistance in air than that of MoSi₂-3.5 vol.% Si₃N₄ coating.

Keywords electron microscopy, heat treatment, intermetallic, x-ray

1. Introduction

Refractory metal molybdenum (Mo) is usually used as a structural material due to its excellent properties, such as high melting point (2620 °C), good corrosion resistance, admirable high-temperature strength and rigidity, and high creep resistance (Ref 1, 2). However, due to the generation of volatile oxide MoO₃, the oxidation resistance of Mo is poor. It is this awful oxidation resistance that hinders the widespread application of Mo and its alloys at high temperatures (Ref 3, 4). In order to broaden the field of Mo applications at high temperatures, different kinds of coatings were fabricated on the surfaces of Mo and its alloys (Ref 5-8). Molybdenum disilicide (MoSi₂) has an excellent high-temperature oxidation resistance, which makes it the most promising coating material for Mo, Nb, and C/C composites (Ref 9-12). The great high-temperature oxidation resistance of MoSi₂ is due to its formation of a protective, glassy

silica (SiO₂) layer on the surface, which blocks oxygen from further intruding into internal of MoSi₂.

For applications of MoSi₂ coating on Mo substrate, one of the biggest challenges was the degradation of MoSi₂ phase at elevated temperatures. In the use of MoSi₂ coating, the SiO₂ and Mo₅Si₃ phases were formed on the surface of the coating. At the meantime, diffusion reaction occurred between MoSi₂ coating and Mo substrate, which resulted in the degradation of interfacial phase MoSi₂ into Mo₅Si₃ and/or Mo₃Si phase. The Mo₅Si₃ layer grew simultaneously in two directions, which led to a rapid decrease in the thickness of the MoSi₂ phase. When MoSi₂ phase completely disappeared, the oxidation reaction was accelerated, since Mo₅Si₃ phases cannot preform as a protective silica layer as MoSi₂ phase did. In this case, the lifetime of MoSi₂ coating depended strongly on the growth of intermediate silicides. Thus, the growth kinetics of the intermediate silicides formed in the MoSi₂/Mo diffusion couples has been extensively investigated to predict the lifetime of MoSi₂ coating (Ref 13-17). Tortorici et al. (Ref 18) found that the Mo₅Si₃ and Mo₃Si layers grew simultaneously with a parabolic rate law at the early annealing stage. Christian et al. (Ref 19) reported that the dominant diffusion element in MoSi₂ was Si, while Yoon et al. (Ref 20) confirmed that Si was a primary diffuser via ZrO₂ marker experiment. These results indicated that the key to increase the lifetime of MoSi₂ coating was to decrease the diffusion rate of Si element. It was found that MoSi₂ composite coatings possessed a better oxidation resistance than single MoSi₂ coating. Wang et al. (Ref 21) developed MoSi₂/MoB composite coating on Mo substrate via chemical vapor deposition and found after 80 h oxidation at 1300 °C in air, the weight gain rate of MoSi₂ single coating was higher than MoSi₂/MoB composite coating. Wang believed that the MoB phase hindered Si element diffusing into Mo substrate and extended the service life of the coating. In our

Houan Zhang, Jia Lin, Ying Chen, and Siyong Gu, Key Laboratory of Functional Materials and Applications of Fujian Province, Xiamen University of Technology, Xiamen, 361024 Fujian, People's Republic of China; and The Key Laboratory for Power Metallurgy Technology and Advanced Materials of Xiamen, Xiamen University of Technology, Xiamen, 361024 Fujian, People's Republic of China; and **Yu Huang**, Xiamen Honglu Tungsten Molybdenum Industry Co. Ltd, Xiamen, 361024 Fujian, People's Republic of China. Contact e-mail: ha_zhang@163.com.

recent works, MoSi₂, MoSi₂-Si₃N₄, and (Mo,W)Si₂-Si₃N₄ coatings were successfully synthesized on Mo substrates through in situ pack cementation (Ref 22, 23). And the (Mo,W)Si₂-Si₃N₄ composite coating exhibited a better oxidation resistance than other two coatings. It was thought that the impediment of Si diffusion by W element contributed to its better oxidation resistance.

The MoSi₂-Si₃N₄/Mo diffusion couples prepared by spark plasma sintering (SPS) were studied in our previous work, suggesting that the addition of Si₃N₄ played a significant role on oxidation properties and microstructures of MoSi₂-Si₃N₄ coating (Ref 24). In the present work, the similar method was carried out to investigate how W element behaved when it was added in MoSi₂-Si₃N₄-WSi₂/Mo diffusion couples. The silicon diffusivity of the Mo₅Si₃ phase was quantitatively calculated on MoSi₂-3.5 vol.% Si₃N₄/Mo and MoSi₂-3.5 vol.% Si₃N₄-*x* vol.% WSi₂ (*x* = 2.0, 4.0, 5.0 and 6.0) diffusion couples annealed at a temperature in the interval between 1200 and 1500 °C. The growth kinetics and silicon diffusion coefficients of intermediate silicides were investigated to improve our understanding on the fundamental mechanism on oxidation resistance by the addition of W element.

2. Experimental Procedures

Commercial MoSi₂ (3-5 μm, purity > 99.5 wt.%), WSi₂ (3-5 μm, purity > 99.5 wt.%), and Si₃N₄ (3-5 μm, purity > 99.5 wt.%) powders were original materials to fabricate the composites. MoSi₂ and 3.5 vol.% Si₃N₄ powders were ball-milled with 2.0, 4.0, 5.0, and 6.0 vol.% WSi₂ powders, respectively, for 10 h in a steel bottle using WC balls within the atmosphere of argon until the powder particles were uniformly distributed. The mixture powders were crushed and passed through a 200-mesh sieve. Mo metal plates (purity > 99.95 wt.%) were cut into pieces of 5 mm × 5 mm × 1 mm and polished with 800 grit SiC papers, then ultrasonically cleaned in ethanol, and dried. Mo plates were settled in the middle of the mixture powders and then filled in a cylindrical graphite die of 30 mm in diameter. The as-received mixtures were sintered in the SPS furnace. The detailed spark plasma sintering procedures were depicted in our previous study (Ref 24). The designation and composition of the samples in this investigation are presented in Table 1.

The SPS diffusion couples were annealed in an alumina tube furnace at temperatures range from 1200 to 1500 °C for various periods of time up to 192 h in Ar atmosphere. The alumina tube was evacuated < 10⁻¹ MPa and backfilled with Ar gas, and these procedures were repeated three times before the annealing treatment. High-temperature oxidation test was conducted at 1450 °C in air for a maximum duration of 384 h. Samples were placed in the hot zone of a furnace in a high-purity alumina crucible. The samples oxidized for a period of time were taken

out from the furnace, followed by cooling to room temperature. The mass change during the high-temperature oxidation was calculated by weighing a balance with a resolution of 0.1 mg.

The surface and cross sections of diffusion couples were polished successively with 400-, 600-, 800-, and 1000-grit SiC papers, then ultrasonically cleaned in ethanol, and dried. The crystalline phases were characterized by x-ray diffraction (XRD, PANalytical X'Pert PRO, Holland). The microstructures were observed by scanning electron microscopy (SEM, ZEISS EVO18, Germany) with simultaneous chemical analysis by energy-dispersive spectroscopy (EDS, Oxford Instrument X-maxN, UK). The thicknesses of intermediate layers formed in diffusion couples were measured by SEM with a micrometer attachment. At least ten measurements were taken for the intermediate layers, and the mean thickness was determined.

3. Results and Discussions

Figure 1 shows XRD patterns taken from the polished surface of MSW5.0/Mo diffusion couple. The XRD patterns of original composite powders before SPS processes were provided as a comparison. It is composed of (Mo,W)Si₂ phase and a small amount of Si₃N₄ and Mo₅Si₃ phases. The peaking positions of (Mo,W)Si₂ solid solution are basically coincident to XRD peaks of MoSi₂ and WSi₂ phases. MoSi₂ and WSi₂ have the similar long-range order structures and the adjacent lattice parameters. When some Mo atoms in MoSi₂ crystals are replaced by W atoms, (Mo,W)Si₂ solid solution is formed. Similarly, the (Mo,W)₅Si₃ solid solution is formed in Fig. 1.

Figure 2 shows the backscattered electron (BSE) images and EDS results taken from the surface of sintered composites. Figure 2(a) shows that in addition to a trace of porosity, the composite is composed of gray (A), gray-white (B), white (C), and black (D) phases. The EDS analysis of point A shows that the gray phase is composed of Mo and Si elements, and the Mo to Si atomic ratio is 1:2.27 in Fig. 2(b), which is closed to stoichiometric ratio of MoSi₂. It is also found in Fig. 2(a) that the gray phase is surrounded by a thin layer of gray-white annular phase (B). The EDS analysis of point B in Fig. 2(c) shows the gray-white phase is composed of Mo, W, and Si elements, and the (Mo,W) to Si atomic ratio of gray-white annular phase is closed to 1:2. This indicates that the crystal grain of the MSW composites after spark plasma sintering shows a special ring-core structure, whose ring is (Mo,W)Si₂ phase and the core is the MoSi₂ phase. Figure 2(d) shows the (Mo,W) to Si atomic ratio of point C is closed to 5:3, which indicates the white phase is (Mo,W)₅Si₃. The EDS analysis of point D shows the round black phase is mainly Si₃N₄ in Fig. 2(e), which is mainly distributed in the grain boundary as described in Ref 25. Obviously, all of the EDS analyses are consistent with the XRD result in Fig. 1.

Table 1 Designation and composition of diffusion couples

Diffusion couples designation	Composition	$K_p, \text{m}^2 \text{s}^{-1} 10^{-14}$
MS3.5/Mo	MoSi ₂ -3.5 vol.% Si ₃ N ₄ /Mo	1.36
MSW2.0/Mo	MoSi ₂ -3.5 vol.% Si ₃ N ₄ -2.0 vol.% WSi ₂ /Mo	1.24
MSW4.0/Mo	MoSi ₂ -3.5 vol.% Si ₃ N ₄ -4.0 vol.% WSi ₂ /Mo	1.14
MSW5.0/Mo	MoSi ₂ -3.5 vol.% Si ₃ N ₄ -5.0 vol.% WSi ₂ /Mo	0.90
MSW6.0/Mo	MoSi ₂ -3.5 vol.% Si ₃ N ₄ -6.0 vol.% WSi ₂ /Mo	1.00

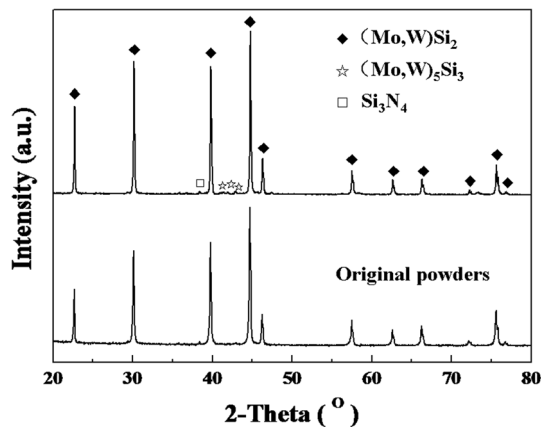


Fig. 1 XRD patterns of the surface of MSW5.0 composite by SPS

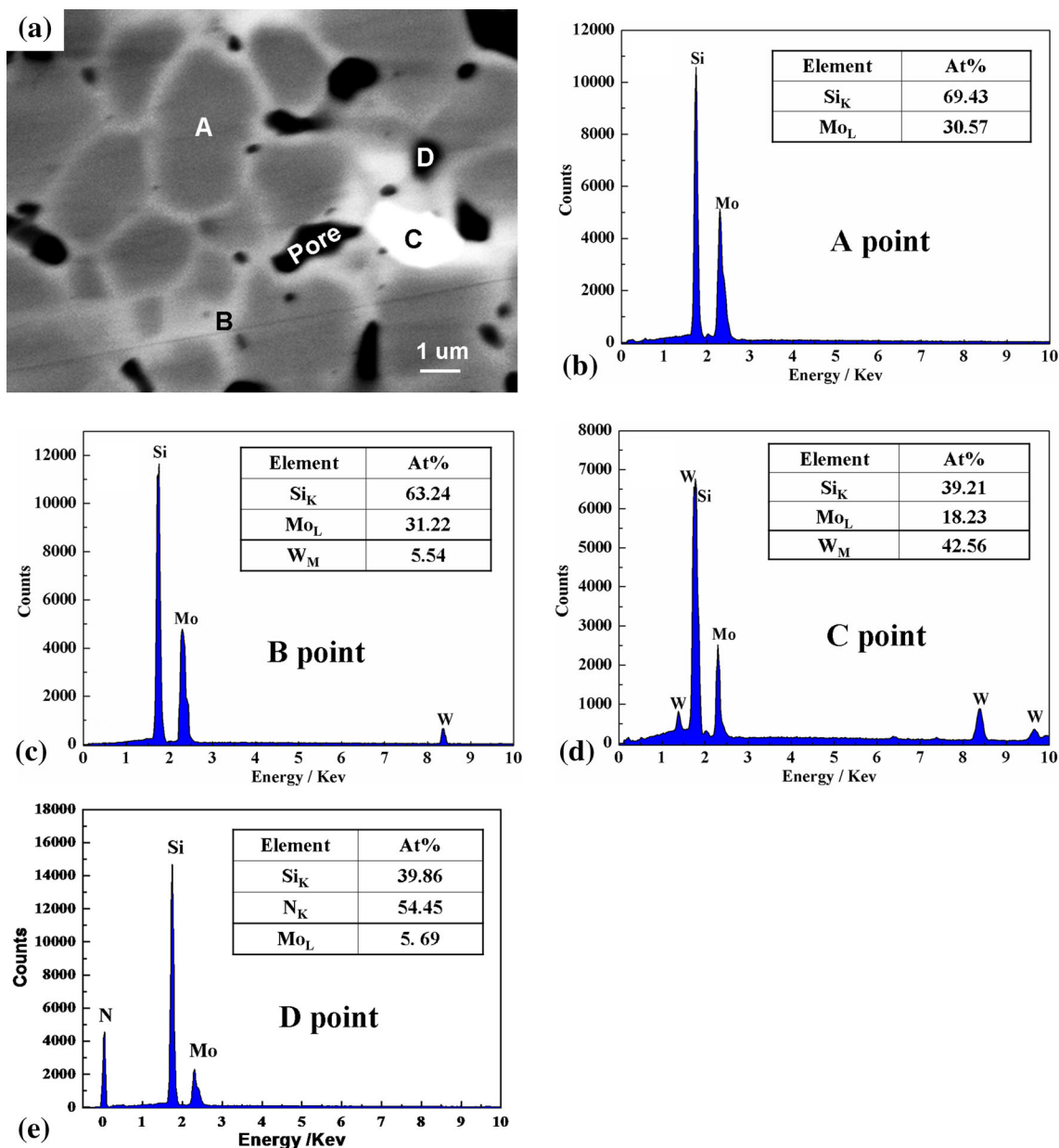


Fig. 2 BSE image and EDS results taken from the MSW composites: (a) a type microstructure, (b) EDS analysis of point A, (c) EDS analysis of point B, (d) EDS analysis of point C, and (e) EDS analysis of point D

Figure 3 shows the BSE images of polished cross sections of annealed diffusion couples. Figure 3(a) shows that in annealing treatment for 24 h, the interfacial region exhibited three different morphologies, and they are marked I, II, and III. I zone is the Mo substrate. III zone contains (Mo,W)Si₂ (the gray phase), Si₃N₄ (the round black phase), and a small amount of (Mo,W)₅Si₃ (the white phase), which is consistent with Fig. 1 and 2. II zone is smooth without pores. The EDS analysis suggests that II zone is the Mo₅Si₃, while W element was not detected. With the annealing treatment time extended to 120 h, a new zone marked IV appears between the II and III. IV zone has similar structures of III zone except more pores. Results from the EDS analysis show the IV zone is (Mo,W)₅Si₃ and the atomic ratio of Mo to W elements in IV region and III region was very close to each other. These phenomena indicated the formation of II zone is attributed to the Si element in the III zone diffusing into Mo substrate and reacting

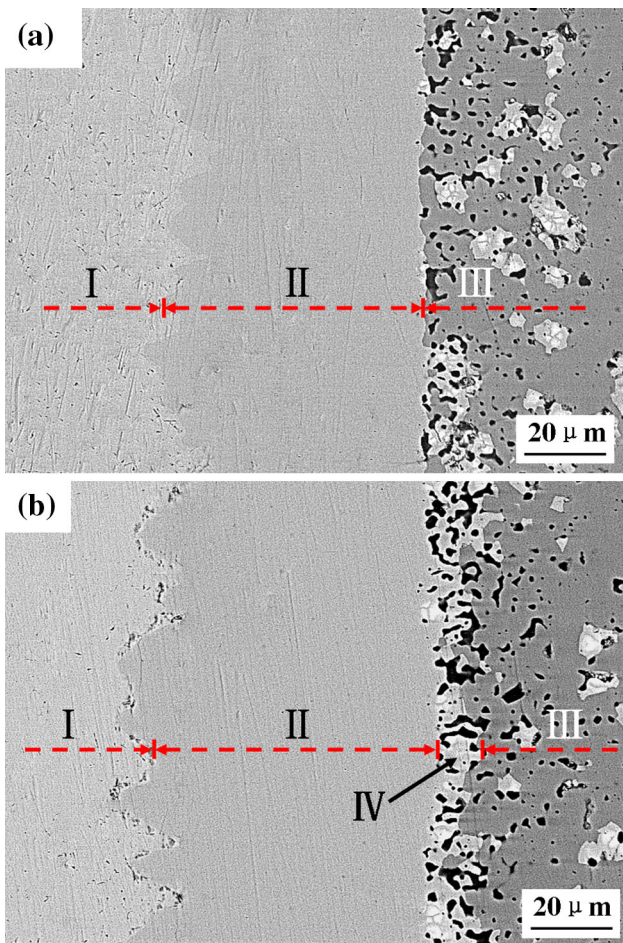


Fig. 3 BSE images of the cross sections of MSW5.0/Mo diffusion couples: (a) annealed for 24 h at 1300 °C; (b) annealed for 120 h at 1300 °C

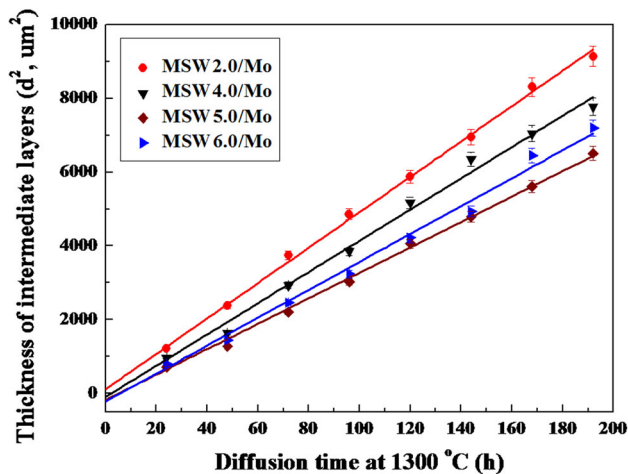


Fig. 4 Thickness of the intermediate layers squared against diffusion time at 1300 °C as functions of WSi₂ content and time

with Mo to form Mo₅Si₃ phase, but the formation of IV zone is attributed to (Mo,W)Si₂ in III zone degrading into (Mo,W)₅Si₃ in IV zone. Two similar different formation mechanisms of Mo₅Si₃ phase are also proved in our previous investigation on MS/Mo diffusion couples (Ref 24). Meanwhile, Fig. 3 shows

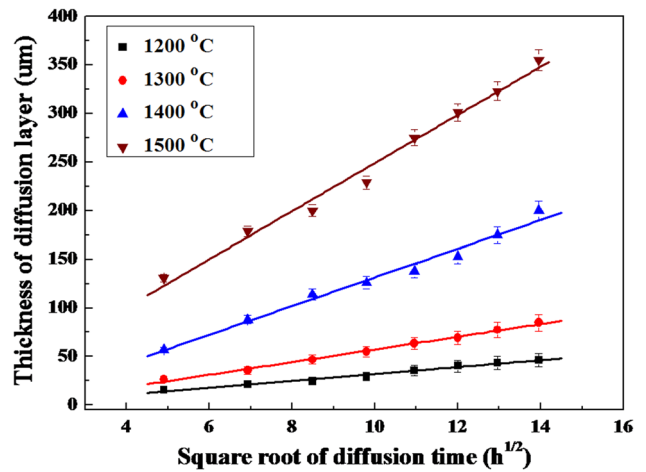


Fig. 5 Thickness of intermediate layers grown in the MSW5.0/Mo diffusion couple as functions of temperature and time

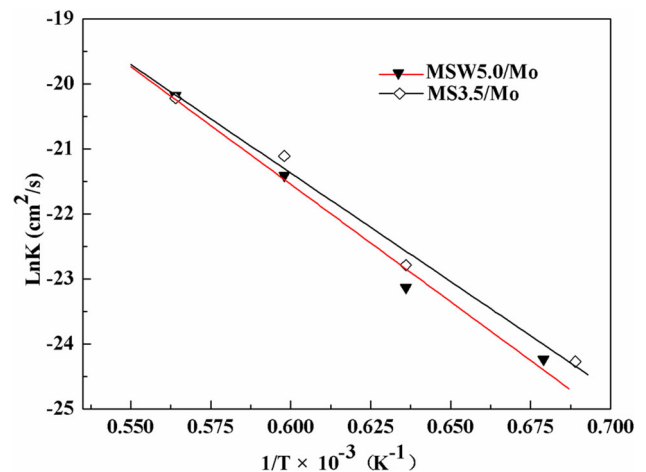


Fig. 6 Arrhenius plots of the parabolic growth constants for Mo₅Si₃ layers obtained in Fig. 5

that the thickness of II zone is obviously higher than that of IV zone. This confirms that Si plays a dominant role in diffusion as referred to in Ref 19 and 20. Reference 26 reported that Si in Mo/MoSi₂ had a higher diffusion rate compared to W in W/WSi₂ diffusion couple, which led to the phenomenon that no W element appeared in II zone.

Thickness of the intermediate layers (Mo₅Si₃) grown in the interface of different diffusion couples is given in Fig. 4 as functions of WSi₂ content and time, where the squared value of thickness was plotted against diffusion time at 1300 °C. The growth rate of intermediate layers obeys the parabolic rate law, of which the parabolic rate constants are determined from the slopes in Fig. 4 and are shown in Table 1. For comparison, the parabolic rate constant of MS3.5/Mo is also shown in Table 1 based on our previous investigation (Ref 24). The parabolic rate constant of intermediate layers is minimum when the WSi₂ content is 5.0 vol.%, which indicates that the intermediate layers in MSW5.0/Mo diffusion couple grow most slowly. Thus, MSW5.0/Mo diffusion couple is selected to carry on the following research.

Figure 5 illustrates the thickness of the diffusion layer increases as the square root diffusion time increases at different

Table 2 Silicon diffusion coefficients in the Mo₅Si₃ of MSW5.0/Mo (D₁) and MS3.5/Mo (D₂) diffusion couples

T, K	D ₁ , cm ² s ⁻¹ 10 ⁻⁹	D ₂ , cm ² s ⁻¹ 10 ⁻⁹
1473	0.140	0.145
1573	0.439	0.619
1673	2.453	3.324
1773	8.042	8.434

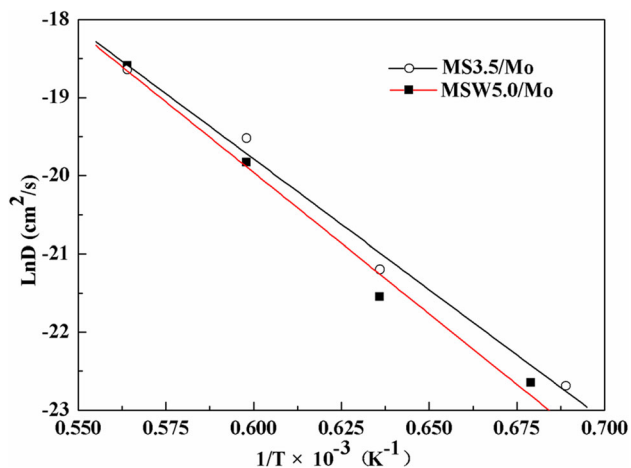


Fig. 7 Temperature dependence for the silicon diffusion coefficient of the Mo₅Si₃ layer of MSW5.0/Mo diffusion couple

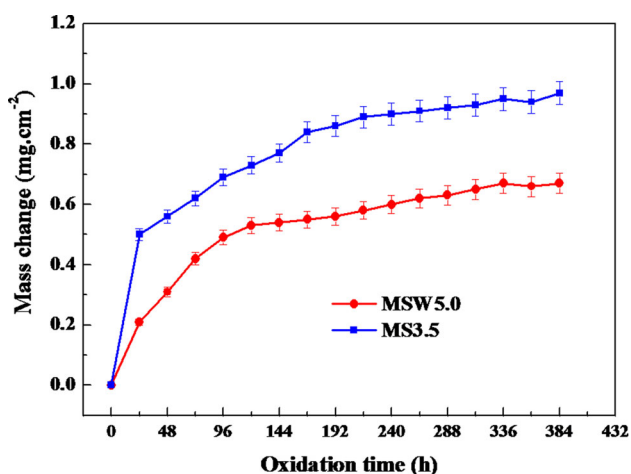


Fig. 8 Mass changes of MS3.5 and MSW5.0 coatings on Mo substrate oxidized at 1450 °C in air

temperature. The parabolic rate constants obtained from Fig. 5 are plotted against reciprocal of an absolute temperature in Fig. 6, where Arrhenius plots for the constants are presented. The kinetic curves of intermediate layers grown in MS3.5/Mo diffusion couples in our previous investigation (Ref 24) are also presented as a comparison in Fig. 6. And the growth rate constants K_p of MSW5.0/Mo and MS3.5/Mo diffusion couples may be well approximately expressed as:

$$K_{p(\text{MSW5.0/Mo})} = 1.15 \exp[-(316 \pm 23)/RT] \quad \text{and}$$

$$K_{p(\text{MS3.5/Mo})} = 0.26 \exp[-(278 \pm 19)/RT].$$

The activation energies for the growth of intermediate layers in MSW5.0/Mo and MS3.5/Mo diffusion couples are 316 ± 23 and 278 ± 19 kJ/mol, respectively.

Silicon diffusion coefficient in the intermediate silicide layers is determined using the parabolic growth constants on the basis of a calculation scheme developed in Ref 15. The effects of Si₃N₄ and WSi₂ on Si concentrations are not the main research aims in this study. However, the concentrations at the coexisting phase boundaries are given referring to Ref 13-15: (Mo,W)Si₂-Si₃N₄/(Mo₅Si₃, (Mo,W)₅Si₃): 66.67/39.1 at.% Si and (Mo₅Si₃, (Mo,W)₅Si₃)/Mo: 37.5/0.1 at.% Si at each temperature. The calculated values are given in Table 2, and the semilogarithmic plots between the silicon diffusion coefficient and a reciprocal of absolute temperature are shown in Fig. 7. Based on numerical simulation, the diffusion coefficient of MSW5.0/Mo (D₁) and MS3.5/Mo (D₂) diffusion couples in 1473-1773 K range can be expressed as: $D_1 = 5.64 \exp[-(316 \pm 23)/RT]$ (cm²/s) and $D_2 = 1.28 \exp[-(278 \pm 19)/RT]$ (cm²/s). Activation energy is the same as obtained for the growth of intermediate layers. This consistency in activation energy is coming from the fact that the composition ranges of both intermediate and MoSi₂ phases are independent to temperatures.

The activation energy of intermediate layers in MSW5.0/Mo diffusion couple is higher about 38 kJ/mol than that of in MS3.5/Mo diffusion couple. Besides, the silicon diffusion coefficient of MSW5.0/Mo diffusion couples is smaller than MS3.5/Mo diffusion couples at the same temperatures. That indicates that the growth of intermediate layers in MSW5.0/Mo diffusion couple is more difficult than that of in MS3.5/Mo diffusion couples. In this case, it is believed that the existence of W element plays the main role in inhibition of the growth of intermediate layers. From Fig. 2, it can be seen that MSW composites have a special ring-core structure, whose ring is (Mo,W)Si₂ phase and the core is the MoSi₂ phase. This means that the Si in both MoSi₂ core and (Mo,W)Si₂ ring in III zone diffuses to II zone and forms Mo₅Si₃ with the Mo substrate, and it must overcome the hindrance role of W-Si bond. However, the crystal binding energy of WSi₂ is higher than that of MoSi₂, and W-Si bond energy (33.397 kJ/mol) is higher than the Mo-Si bond energy (26.420 kJ/mol) in Ref 27. Chatilyan et al. (Ref 17) compared Si diffusion coefficient and diffusion activation energy in the MoSi₂ and WSi₂ at the range of 850-1500 °C. It was also found that the diffusion coefficient of Si in the WSi₂ is lower than that in MoSi₂ and the diffusion activation energy of Si in the WSi₂ is higher than that in MoSi₂. The results of the above study indicate that it is more difficult for Si to break away from the constraint of W-Si bond than Mo-Si bond, and Si diffusion is more difficult in WSi₂ than in MoSi₂. Therefore, MSW5.0/Mo diffusion couple exhibits higher activation energy and lower silicon diffusion coefficient than that of MS3.5/Mo diffusion couple.

The mass variation of MS3.5 and MSW5.0 coatings on Mo substrate oxidized at 1450 °C in air is illustrated in Fig. 8. As it can be seen, the mass weighting of MSW5.0 coating is lower than that of MS3.5 coating. It gives an actual evidence of WSi₂ blocking the diffusion of Si. As the results calculated in previous section, MSW5.0 coating has lower silicon diffusion

coefficient and higher activation energy for the growth of intermediate layers compared with that of MS3.5 coating. This causes a lower growth rate constant of intermediate layers in MSW5.0 coating and results in MSW 5.0 coating on Mo substrate having a better high-temperature oxidation resistance than that in MS3.5 coating.

4. Conclusions

The microstructure evolutions, growth rate constants, and silicon diffusion coefficients of intermediate silicide phases in MoSi₂-3.5 vol.% Si₃N₄-x vol.% WSi₂/Mo (x = 2.0, 4.0, 5.0 and 6.0) by SPS were investigated at temperatures range from 1200 to 1500 °C. The results are summarized as follows:

1. A special microstructure with MoSi₂ core surrounded by a thin layer of (Mo,W)Si₂ ring is found in the MSW composites. The intermediate layers of Mo₅Si₃ at early diffusion stage and (Mo,W)₅Si₃ at late diffusion stage in MoSi₂-Si₃N₄-WSi₂/Mo diffusion couple are formed. Mo₅Si₃ is resulted from the diffusion reaction of Si with the Mo substrate, and (Mo,W)₅Si₃ is attributed to the degrading of (Mo,W)Si₂.
2. The growth of intermediate layers in MoSi₂-Si₃N₄-WSi₂/Mo diffusion couple is confirmed to obey the parabolic law. The growth rate constant of intermediate layer in this diffusion couples is minimum when the content of WSi₂ was 5.0% in volume.
3. Compared with MS3.5/Mo diffusion couple, MSW5.0/Mo diffusion couple has higher about 38 kJ/mol of activation energy for the growth of intermediate layers and lower silicon diffusion coefficient. It indicates the obvious hindering effect of WSi₂ in the MSW composite on Si diffusion. MSW5.0 coating on Mo substrate exhibits a better high-temperature oxidation resistance in air than that of MS3.5 coating.

Acknowledgments

This project was financially supported by the National Natural Science Foundation of China (No. 51371155), the Key Science and Technology Project of Fujian Province of China (No. 2014H0046), the Scientific Research Fund of Xiamen City of Fujian Province of China (No. 3502ZZ20143036), and the Education Department Science and Technology Project of Fujian Province of China (No. JB13149).

References

1. F. Jiang, Y. Zhang, N. Sun, and J. Leng, Tungsten Coating Prepared on Molybdenum Substrate by Electrodeposition from Molten Salt in Air Atmosphere, *Appl. Surf. Sci.*, 2015, **327**, p 432–436
2. K. Babinsky, J. Weidow, W. Knabl, A. Loriclf, H. Leitner, and S. Primig, Atom Probe Study of Grain Boundary Segregation in Technically Pure Molybdenum, *Mater. Charact.*, 2014, **87**, p 95–103
3. L. Dai, Y. Yu, H. Zhou, X. Yan, J. Zhu, Y. Li, and L. Wang, In-Situ Synthesis of MoSi₂ Coating on Molybdenum Substrate by Electro-Deoxidation of a SiO₂ Layer in Molten Salt, *Ceram. Int.*, 2015, **41**, p 13663–13670

4. X. Tian, X. Guo, Z. Sun, Z. Yin, and L. Wang, Formation of B-Modified MoSi₂ Coating on Pure Mo Prepared Through HAPC Process, *Int. J. Refract. Met. Hard Mater.*, 2014, **45**, p 8–14
5. S. Majumdar, Formation of MoSi₂ and Al Doped MoSi₂ Coatings on Molybdenum Base TZM (Mo-0.5Ti-0.1Zr-0.02C) Alloy, *Surf. Coat. Technol.*, 2012, **206**, p 3393–3398
6. B. Paul, P.K. Limaye, R.C. Hubli, and A.K. Suri, Microstructure and Wear Properties of Silicide Based Coatings Over Mo-30W Alloy, *Int. J. Refract. Met. Hard Mater.*, 2014, **44**, p 77–83
7. Y. Niu, H. Wang, Z. Liu, C. Hu, X. Wang, X. Zheng, and C. Ding, Microstructure Evolution of ZrB₂-MoSi₂ Composite Coatings at Middle and High Temperatures, *Surf. Coat. Technol.*, 2015, **273**, p 30–38
8. J. Liu, Q. Gong, Y. Shao, D. Zhuang, and J. Liang, In-Situ Fabrication of MoSi₂/SiC-Mo₂C Gradient Anti-Oxidation Coating on Mo Substrate and Crucial Effect of Mo₂C Barrier Layer at High Temperature, *Appl. Surf. Sci.*, 2014, **308**, p 261–268
9. Y. Wang, D.Z. Wang, J.H. Yan, and A.K. Sun, Preparation and Characterization of Molybdenum Disilicide Coating on Molybdenum Substrate by Air Plasma Spraying, *Appl. Surf. Sci.*, 2013, **284**, p 881–888
10. P. Zhang and X. Guo, Preparation and Oxidation Resistance of Silicide/Aluminide Composite Coatings on an Nb-Ti-Si Based Alloy, *Surf. Coat. Technol.*, 2015, **274**, p 18–25
11. B.A. Gnesin, I.B. Gnesin, and A.N. Nekrasov, The Silicide Coatings (Mo,W)Si₂ + (Mo,W)₅Si₃ on Graphite, Interaction with Carbon, *J. Alloys Compd.*, 2013, **549**, p 308–318
12. T. Feng, H.J. Li, S.L. Wang, M.H. Hu, and L. Liu, Boron Modified Multi-layer MoSi₂-CrSi₂-SiC-Si Oxidation Protective Coating for Carbon/Carbon Composites, *Ceram. Int.*, 2014, **40**, p 15167–15173
13. P.C. Tortorici and M.A. Dayananda, Interdiffusion and Diffusion Structure Development in Selected Refractory Metal Silicides, *Mater. Sci. Eng. A*, 1999, **261**, p 64–77
14. F. Christian, H. Sohma, T. Tanaka, H. Tanaka, K. Ohsasa, and T. Narita, Growth Rate Constant and Chemical Diffusivity in Silicides Mo₅Si₃ and Ta₅Si₃, *Mater. Trans. JIM*, 1998, **2**, p 286–291
15. H.A. Chatilyan, S.L. Kharatyan, and A.B. Harutyunyan, Diffusion Annealing of Mo/MoSi₂ Couple and Silicon Diffusivity in Mo₅Si₃ Layer, *Mater. Sci. Eng. A*, 2007, **459**, p 227–232
16. J.H. Yan, Y. Wang, L.F. Liu, and Y. Wang, Oxidation and Interdiffusion Behavior of Niobium Substrate Coated MoSi₂ Coating Prepared by Spark Plasma Sintering, *Appl. Surf. Sci.*, 2014, **320**, p 791–797
17. H.A. Chatilyan, L.H. Arakelyan, and S.L. Kharatyan, Growth Kinetics and Silicon Diffusivity in MoSi₂ and WSi₂ Disilicides, *Defect Diffus. Forum*, 2005, **237-240**, p 867–872
18. P.C. Tortorici and M.A. Dayananda, Diffusion Structures in Mo Vs. Si Solid-Solid Diffusion Couples, *Scr. Mater.*, 1998, **38**, p 1863–1869
19. F. Christian and T. Narita, Siliconizing of Molybdenum Metal in Indium-Silicon Melts, *Mater. Trans.*, 1998, **39**, p 658–662
20. J.Y. Byun, J.K. Yoon, G.H. Kim, J.S. Kim, and C.S. Choi, Study on Reaction and Diffusion in the Mo-Si System by ZrO₂ Marker Experiments, *Scr. Mater.*, 2002, **46**, p 537–542
21. Y. Wang, D. Wang, and J. Yan, Preparation and Characterization of MoSi₂/MoB Composite Coating on Mo Substrate, *J. Alloys Compd.*, 2014, **589**, p 384–388
22. S.Y. Gu, H.A. Zhang, and N.P. Xie, Oxidation Property of MoSi₂-Si₃N₄ Coating on Mo Substrate, *J. XMUT*, 2011, **19**, p 18–21
23. H. Zhang, J. Lv, Y. Wu, S. Gu, Y. Huang, and Y. Chen, Oxidation Behavior of (Mo,W)Si₂-Si₃N₄ Composite Coating on Molybdenum Substrate at 1600 °C, *Ceram. Int.*, 2015, **41**, p 14890–14895
24. Y. Huang, J. Lin, and H. Zhang, Effect of Si₃N₄ Content on Microstructures and Antioxidant Properties of MoSi₂/Si₃N₄ Composite Coatings on Mo Substrate, *Ceram. Int.*, 2015, **41**, p 13903–13907
25. J.K. Yoon, G.H. Kim, J.Y. Byun, J.K. Lee, Y.H. Paik, and J.S. Kim, Formation of MoSi₂-Si₃N₄ Composite Coating by Reactive Diffusion of Si on Mo Substrate Pretreated by Ammonia Nitridation, *Scr. Mater.*, 2002, **47**, p 249–253
26. S. Roy and A. Paul, Diffusion in Tungsten Silicides, *Intermetallics*, 2013, **37**, p 83–87
27. K. Peng, M. Yi, L. Ran, and Y. Ge, Effect of W Addition Content on Valence Electron Structure and Properties of MoSi₂-Based Solid Solution Alloys, *Mater. Chem. Phys.*, 2011, **129**, p 990–994